Journal of Engineering Science and Technology
Vol. 6, No. 3 (2011) 369 - 381

AN INVESTIGATION ON THE AERODYNAMIC CHARACTERISTICS OF 2-D AIRFIOL IN GROUND COLLISION

HUSSAIN H. AL-KAYIEM*, AK KARTIGESH A/L KALAI CHELVEN

Mechanical Engineering Department,UniversitiTeknologi PETRONAS,
31750 Tronoh, Perak, Malaysia
*Corresponding Author: hussain_kayiem@petronas.com.my

Abstract

Near ground operation of airplanes represents a critical and an important aerodynamic practical problem due to the wing-ground collision. The aerodynamic characteristics of the wing are subjected to dramatic changes due to the flow field interference with the ground. In the present paper, the wing-ground collision was investigated experimentally and numerically. The investigation involved a series of wind tunnel measurements of a 2-D wing model having NACA4412 airfoil section. An experimental set up has been designed and constructed to simulate the collision phenomena in a low speed wind tunnel. The investigations were carried out at different Reynolds numbers ranging from 10^5 to 4×10^5, various model heights to chord ratios, *H/C* ranging from 0.1 to 1, and different angles of attack ranging from -4^o to 20^o. Numerical simulation of the wing-ground collision has been carried out using FLUENT software. The results of the numerical simulation have been validated by comparison with previous and recent experimental data and it was within acceptable agreement. The results have shown that the aerodynamic characteristics are considerably influenced when the wing is close to the ground, mainly at angles of attacks 4^o to 8^o. The take off and landing speeds are found to be very influencing parameters on the aerodynamic characteristics of the wing in collision status, mainly the lift.

Keywords: NACA4412, Airfoil Section, Collision, Aerodynamic characteristics, Wings, Wing in ground effect.

1. Introduction

One of the most practical problems, in flight operation, is the wing ground interference, or what is called 'collision', during take off and landing of aircrafts. The aerodynamic characteristics of the wing are changing in the collision phenomena. Aircraft (A/C) performance during take off and landing is influenced

Nomenclatures

A/C	Aircraft
AOA	Angle of attack, deg.
C	Chord length, m or mm
$C_{d,}$	Drag coefficient
C_l	Lift coefficient
C_m	Pitching moment coefficient
H/C	Height to chord ratio
p	Pressure, N/m^2
Re	Reynolds number
u	Velocity component in x-axis, m/s
v	Velocity component in y-axis, m/s
x,y	Axial and transverse axes

Greek Symbols

α	Angle of attack, deg.
μ	Air viscosity, kg/m.s
ρ	Air density, kg/m^3
σ	Shear stress, N/m^2

due to the influence in the aerodynamic factors of the wing, where near the ground, the flow field structure around any flying body is disturbed due to the interference with the ground.

Among various literatures that describe the flow field around the A/C wings, related the lift generation with induced drag due to vortex generation [1]. When producing lift, a wing generates strong swirling masses of air off both its wingtips. As the wing moves forward, this vortex remains, and therefore trails behind the wing. For this reason, the vortex is usually referred to as a trailing vortex. One trailing vortex is created off each wingtip, and they spin in opposite directions. Besides generating lift, the trailing vortices also have their primary effect that deflecting the flow behind the wing downward. This induced component of velocity, which is called downwash, reduces the amount of lift produced by the wing. In order to make up for that lost lift, the wing must go to a higher AOA and this increase in angle of attack increases the drag generated by the wing. Such drag is named 'induced drag' because it is induced by the process of creating additional lift. The phenomenon is most often observed when an airplane is landing, and pilots often describe a feeling of "floating" or "riding on a cushion of air" that forms between the wing and the ground [2]. The effect of this behaviour is to increase the lift of the wing and make it more difficult to land. However, there is no "cushion of air" holding the plane up and making it "float." What happens in reality is that the ground partially blocks the trailing vortices and decreases the amount of downwash generated by the wing. This reduction in downwash increases the effective angle of attack of the wing so that it creates more lift than it would otherwise. This phenomenon is called the wing in ground effect.

Hsuin and Chen [3] have studied numerically the influence of the aerodynamic characteristics of a 2-D airfoil with ground effect. They have used the standard k-ε turbulence model and solved Navier-Stokes equations by finite volume method using grid generation program developed by the authors, and the PHOENICS code. The analysis covered an operational range of $2\times10^5<Re<2\times10^6$. Zerihan and Zhang [4] have investigated the performance characteristics and the flow field of WIG effect in low speed wind tunnel with moving ground. The wing model is a highly cambered airfoil. They found that at clearance, H/C less than 10%, the down force drops as the wing is stalled. Zhang and Zarihan [5] used LDA and particle image velocimetry to investigate the turbulent wake and edge vortex in WIG fly conditions. They concluded that as the wing height is reduced, separation occurred on the suction surface and the span wise vortex shedding is found to have flip flop nature.

Firooz and Gadami [6] have carried out numerical analysis of the flow field and the aerodynamic characteristics of NACA4412 airfoil in unbounded flow and in collision with ground. The simulation was carried out at 6^o AOA. They have presented results of the lift, drag, pressure and friction coefficients at various heights to chord ratios, H/C = 0.08, 0.1, 0.2, 0.3, 0.5, 0.8, and far from ground. Their results have shown that as the airfoil approach the ground, the lift coefficient was increased, while the drag, pressure, and friction coefficients were reduced.

A widely covered background on the WIG is presented by Ahmed et al. [7]. It could be concluded from their literature survey that the wing collision phenomena was studied under Re ranging from 2.4×10^5 to 2×10^6. In their experimental and numerical investigation, they have studied the 2-D NACA4412 WIG at Re = 3×10^5. Prior to [7], Ahmed and Sharma [8] have reported results on the symmetrical NACA0015 airfoil in ground at Re = 2.4×10^5, which obtained from experimental measurements for H/C = 0.05 to 1 and an AOA = 0^o to 12^o. Ahmed, Ahmed [9] reported experimental results on NACA4415 at Re = 2.4×10^5 for AOA = 0^o to 10^o, and H/C = 0.05 to 1 with fixed ground test section.

Molina and Zhang [10] have extended the investigations by study the WIG phenomena with oscillation. They have studied numerically the aerodynamic behaviour of an inverted airfoil by imposing a sinusoidal movement normal to the free stream. They found that the down force is related to the vertical acceleration of the airfoil.

Most of the previous similar investigations were found to be carried out at one Re value. In the present work, the aerodynamic characteristics of aircraft wings in collision fly operation were investigated at variable range of Re. NACA4412 airfoil was selected for profiling the wing section. The investigation was carried out experimentally, in a low speed wind tunnel, and numerically, by CFD analysis using FLUENT version 6-3.26 software assuming 2-D flow field. The practical operational parameters near ground flight, like the fly speed and the AOA, were identified to simulate the flow field around the wing, and the influence of the lift force, the drag force, and the pitching moment were investigated. The investigation covered a range of Re = 10^5 to 4×10^5, and clearance range of $0.1<H/C<1.0$. The tests were extended to cover large range of AOA ranging from -4^o to 20^o.

2. Experimental Verification

2.1. Experimental setup

The experimental tests were conducted in low speed subsonic wind tunnel having test section with 300 mm x 300 mm cross section. The flow velocity in the test section could be varied up to 60 m/s. A special holding mechanism was designed and fabricated to permit variation in the height of the airfoil model from the lower surface of the test section. The holding mechanism was connected to an electronic three weight balance unit in the underneath of the test section, as shown in Fig. 1.

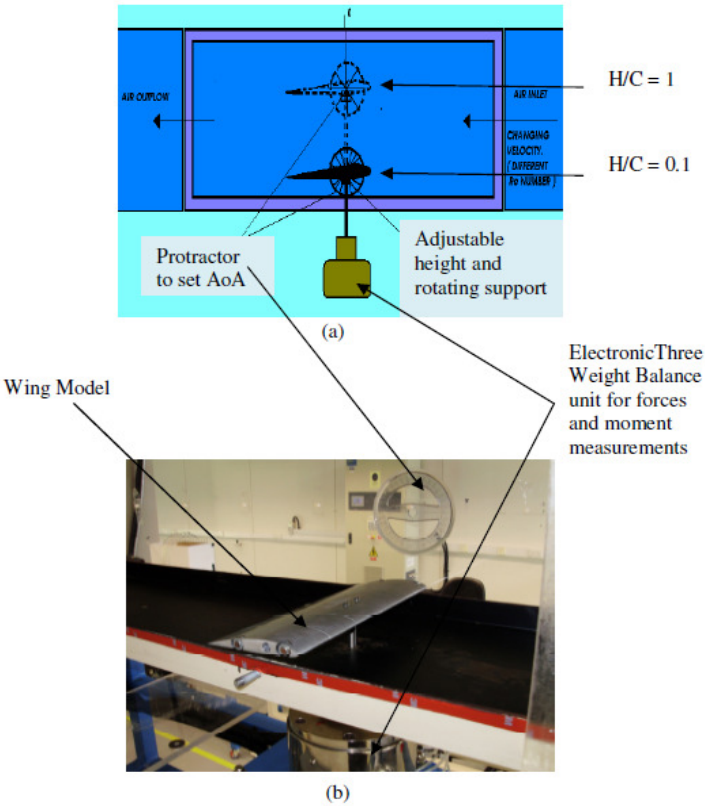

Fig. 1. (a) Schematic of Side-view of the Test Section, (b) the Actual Arrangement of the Model in the Test Section.

2.2. Wing model

The 2-D wing model selected for the present investigation has NACA4412 airfoil section with 105 mm chord length and 300 mm. The profile was obtained by running FoilDesign software and the surface points were fed to CNC machine. The production procedure of the model is discussed in details by Al-Kayiem and Aziat [11]. The airfoil was subjected to finishing accuracy test by using Laser Surface Digitizer. The maximum error between the digitization results and the standard data of the airfoil was 3%. The model was mounted spanning the entire 300 mm width of test section.

At one side of the model, a protractor was attached and used to set the model at the appropriate angle of attack. Another scale with 1 mm divisions was used to measure the airfoil height over the lower surface of the test section.

2.3. Experimental procedure

Prior to each test, the three weight balance system was calibrated according to the manufacturer specified procedure to measure the aerodynamic parameters, lift and drag forces and the pitching moment. For each test, the fan speed was set to provide velocity corresponding to the desired Re. The airfoil was adjusted first to -4^o AOA and a height correspond to H/C = 0.1. Three readings of each aerodynamic parameter were recorded, via PC online interfacing, and the average value was considered. Then, the height was increased to 0.2 and the same way is used for the aerodynamic parameters measurements. The same procedure was repeated for the other pre-selected heights up to H/C = 1. The AOA adjusted to 0^o and the same measurement was obtained for the entire settings of the heights. Similarly, all the aerodynamic parameters were measured over the range of AOA up to 20^o.

3. Numerical Analysis

In the aerodynamic studies, whether it is theoretical, experimental or computational, all efforts are normally aimed at one objective: to determine the aerodynamic forces and moments acting on a body moving through air. The main purpose of employing CFD here is to predict the aerodynamic forces: lift and drag, and the pitching moments, acting on the wing, with reduced time and cost, compared with the experimental tests.

The numerical analysis was based on the discretization of the domain and the governing equations of the flow field. For the present 2-D, steady, incompressible, viscous analysis, the mass and momentum conservation principles were applied as derived from Navier-Stokes equations [12], as:

$$\left(\frac{\partial u}{\partial x}+\frac{\partial v}{\partial y}\right)=0 \tag{1}$$

$$\rho\left(u\frac{\partial u}{\partial x}+v\frac{\partial u}{\partial y}\right)=-\frac{\partial p}{\partial x}+\mu\left(\frac{\partial^2 u}{\partial x^2}+\frac{\partial^2 u}{\partial y^2}\right)+S_{b,x} \tag{2}$$

$$\rho\left(u\frac{\partial v}{\partial x}+v\frac{\partial v}{\partial y}\right)=-\frac{\partial p}{\partial y}+\mu\left(\frac{\partial^2 v}{\partial x^2}+\frac{\partial^2 v}{\partial y^2}\right)+S_{b,y} \tag{3}$$

where, $S_{b,x}$ and $S_{b,y}$ are the body forces in x and y directions, respectively.

3.1. Boundary conditions

To stabilize the prediction of the forces and moment, the flow field surrounding the airfoil was select as 9C in the flow direction times 5C in the transverse direction. The inflow was selected as 3C, the outflow as 5C and the far flow

above the model as 4C and the underneath as 1C. By taking the first point of leading edge nose circle as the origin (0, 0), the resulting computational domain are shown in Fig. 2 below.

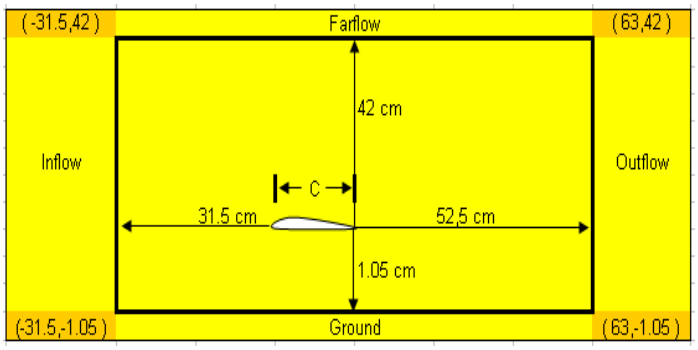

Fig. 2. The Model Setup and the Boundary Conditions Adopted for the CFD Simulation at AOA = 0°.

3.2. Grid generation

The field was meshed using the volume meshing tool. Only one element type was sucessfully applied that is the quadrilatral type. The mesh was unstructured type, as shown in Fig. 3. The advantage of selecting non structured type was mainly due to the complexity of the airfoil profile, and also to allow mesh refinment near the body surface and the highly turbulated regions. The selected elements were QUAD 8-node which are quadrilatral elements with mid edge nodes. Errors were received when attmpteing to use any other element type. The mesh was refined gradually to prove the grid independency. The total number of elements was 7,115 elments.

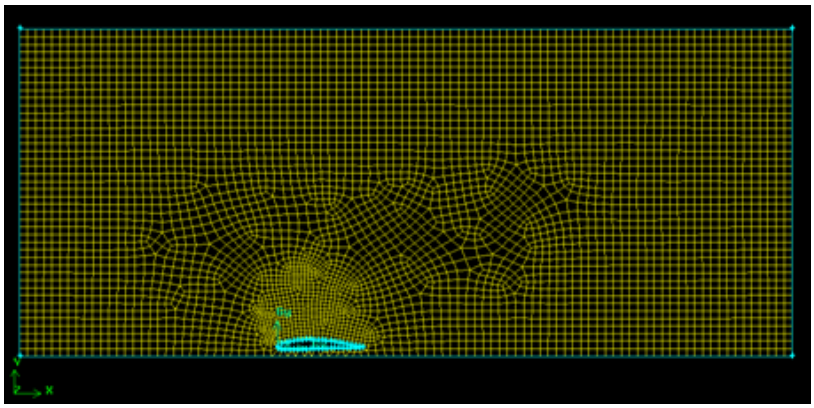

Fig. 3. The Unstructured Generated Grid with QUAD 8-nodes Option in GAMBIT.

3.3. Numerical simulation

The simulation of the flow was carried out by running FLUENT software under the same operational conditions of the experiments. The body forces were neglected due to the low gas weight compared with other forces.

3.4. Turbulent model

For the two dimensional, steady, incompressible, and turbulent viscous flow, the mass and momentum equations cauld be written in the Reynolds-Averaged Navier-Stokes (RANS) as [13]:

$$\frac{\partial u}{\partial x}+\frac{\partial v}{\partial y}=0 \tag{4}$$

$$\rho\frac{\partial}{\partial x}(uv)=-\frac{\partial p}{\partial y}+\frac{\partial}{\partial x}\left[\mu\left(\frac{\partial v}{\partial x}+\frac{\partial u}{\partial y}-\frac{2}{3}\tau_{yx}\frac{\partial v}{\partial y}\right)\right]+\rho\frac{\partial}{\partial x}(\overline{-u'v'}) \tag{5}$$

$$\rho\frac{\partial}{\partial y}(uv)=-\frac{\partial p}{\partial x}+\frac{\partial}{\partial y}\left[\mu\left(\frac{\partial u}{\partial y}+\frac{\partial v}{\partial x}-\frac{2}{3}\tau_{xy}\frac{\partial u}{\partial x}\right)\right]+\rho\frac{\partial}{\partial y}(\overline{-u'v'}) \tag{6}$$

where the velocity components in x-direction, u, the velocity component in y-direction,v and the pressure, p are decomposed into the mean ($\bar{}$), and the fluctuating components, ($'$) as:

$$u=\bar{u}+u', \qquad v=\bar{v}+v', \qquad \text{and} \qquad p=\bar{p}+p' \tag{7}$$

The variables in Eqs. (4)-(6) are representing the time averaged values, with additional term represents the turbulence, or the fluctuating part in the velocity components, as $(\overline{-u'v'})$.

In the solution of the conservation equations, the turbulence term should be replaced by suitable equivalent model; otherwise, the equations are not solvable. The model used to solve the simulation is the renormalization group theory, RNG k-ε model. This model is similar to the standard k- ε with some additional advantages. It improve the accuracy of the results by inclusion of the swirl which is for no doubt exist in the flow field over the wings, and also, the turbulent Prandtl number is evaluated analytically, in contrast to the standard model which uses the user specified constant value.

4. Results

In the present work, the collision is investigated experimentally and numerically. 2-D, NACA4412 airfoil section was selected to model the wing. The results were obtained from variation of the following parameters:

- In the study of collision, one of the main parameters which should be considered is the height-to chord (*H/C*) ratio. The term height, *H* here refers to the clearance between the ground surface and the lowest point of the airfoil or the wing. *H/C* in the present work is selected as 0.1, 0.2, 0.4, 0.6, 0.8, and 1.0.

- It is known that the aerodynamic forces created on flying bodies in viscid flow are originated from the shear and normal stresses distributed over the surface of the body. Representation of viscous forces is best identified Re. Accordingly, Re was varied in this work over range from10^5 to 4×10^5, which is close to the actual operational Re at take off and landing.
- It is quite common to represent the aerodynamic characteristics of an airfoil section by measuring the lift, drag and pitching moment coefficients at different AOA. In the present work, the influence in each coefficient due to collision was estimated at -4.0°, 0.0°, 4.0°, 8.0°, 12.0°, 16.0°, and 20.0° angles of attack.
- The design operational angle of attack for NACA4412 is around $4^o<AOA<10^o$, where the highest lift to drag is produced in this range of AOA. Also, this operating range is safe since it is below the stall limit for NACA4412, even for low Re. Accordingly, the analyses of results would focus on the results obtained at 4° and 8° AOAs.

In the CFD simulation, default convergence criteria were used where it is set at 0.001 for all quantities except for the energy which was set to 10^{-6}. Convergence was reported after 150 to 180 iterations. The grid dependency was also considered by varying the number of the diecretization elements.

5. Results

5.1. Lift results

Figures 4(a) and 4(b) are showing the results of the lift coefficients at 4° and 8° AOA, respectively, as obtained from the experimental and numerical simulation. Also, the results obtained by Firooz and Gadami [6] are included for comparison and validation. Quite good agreement between the experimental and numerical results could be realized. At AOA = 8°, the lift coefficient values at *H/C* = 0.1 are about 10% higher than their values as the wing departure from the ground, up to about *H/C* = 0.8. When the distance increased to *H/C* = 1, the lift, as measured experimentally, tends to increase and approach the normal operation at far away from the ground. This means that the air cushion collision is terminated. The trend of the lift reduction in, the case of 4°, continue even after *H/C* was larger than 0.8.

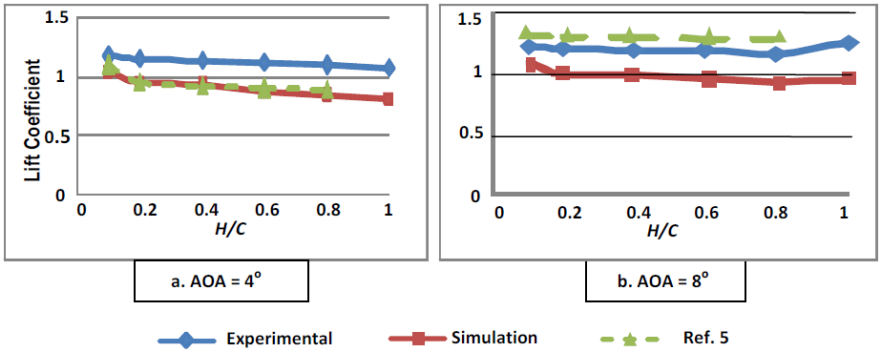

Fig. 4. Variation of the Lift Coefficient with the Wing-Ground Distance at Re = 4×10^5.

The variation of the lift coefficient within the operational limit of Re is shown in Fig. 5. Within $10^5 < Re < 3.5\times10^5$, a high agreement between the measured and the predicted values of the lift coefficient was noticed. As the speed increased to so that $Re > 3.5\times10^5$, the lift predicted values by the simulation were observed to be slightly higher than the measured values.

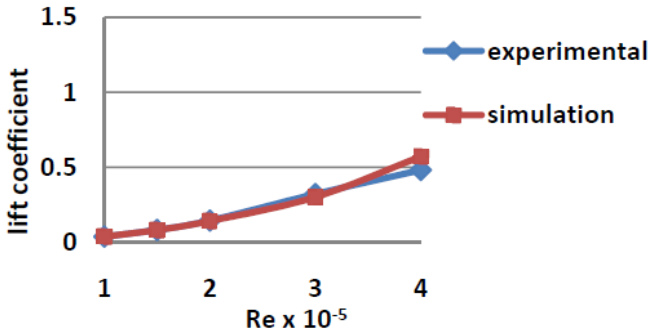

Fig. 5. Variation of the Measured and Predicted Lift Coefficient within the Operational Range of Re (AOA = 4°, *H/C* = 0.1).

5.2. Drag results

The variation of the drag coefficients with the distance from the ground are shown in Figs. 6(a) and 6(b) for 4° and 8° AOAs, respectively. The simulation predicted slightly higher value than the experimental measured results. The trend of the variation was similar in the experimental and simulation analysis; which is similar to the results reported by [6]. For $0.2<H/C< 0.8$, the drag was reduced to its minimal values; while, for $0.2>H/C< 0.8$, it has shown higher values.

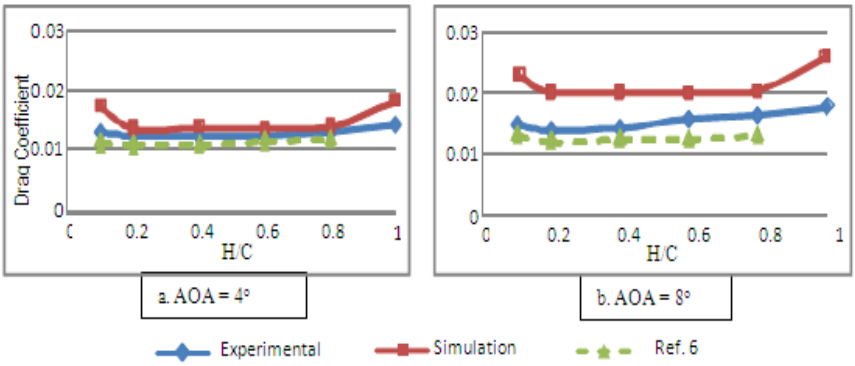

Fig. 6. Variation of the Drag Coefficient with the Wing-Ground Distance at Re = 4×10^5.

Figure 7 shows the drag coefficient values as obtained from the experimental measurements and the CFD simulation. Similar to the case of the lift, the simulation overestimate the drag coefficient values at $Re > 3.5 \times 10^5$. It should be highlighted here that the drag coefficient was increased dramatically (about 80%) as the Re increased from 10^5 to 4×10^5.

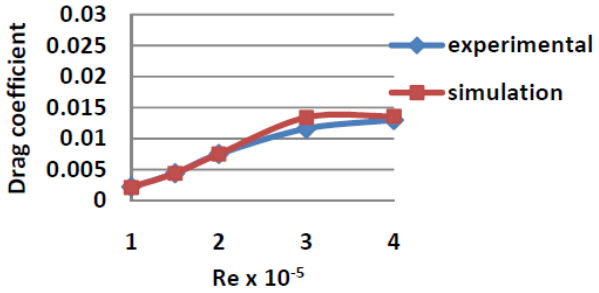

Fig. 7. Variation of the Measured and Predicted Values of the Drag Coefficient within the Operational Re Range (A0A = 4°, *H/C* = 0.1).

5.3. Pitching moment results

The results of the pitching moment obtained from the wind tunnel measurements and the CFD simulation are presented in Fig. 8 as coefficient at various Re. Very close results could be noticed in the low operatinal range of Re, up to 3×10^5. Higher than this Re limit, the predicted values deviated from the measured values. The simulation results were found to be lower than the experimental results. This may due to the enlargement of the reversal flow over the wing which increased the turbulence contribution in the exact solution. experimental measurements errors, which increases slghtely at higher wind speed.

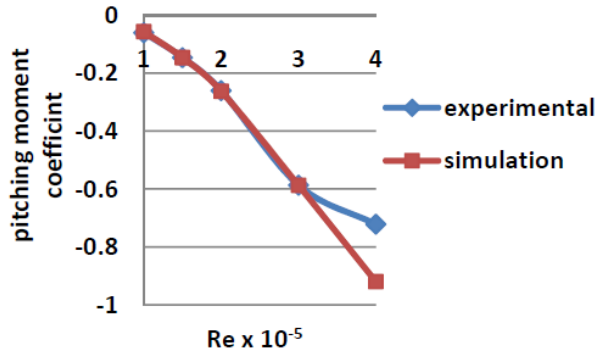

Fig. 8. Variation of the Measured and Predicted Values of the Pitching Moment Coefficient within the Operational Re range (A0A = 4°, *H/C* = 0.1).

5.4. Computational visualization

Another advantage of using CFD is its ability to perform flow visualization. Air being invisible, under normal circumstances, the human's naked eye is unable to see how the air behaves. Typically, flow visualization is being carried out either in a smoke tunnel or water tunnel. But with CFD, flow can be visualized by analyzing the velocity vector plots and tracking the particles that being injected into the simulation. Observing the flow patterns will enable a better understanding of the physics of the flow. The CFD visual experimental set-up was modelled using GAMBIT software with the boundaries shown in Fig. 2.

Some qualitative results were obtained from the simulation as velocity contours and pressure contours, for various cases of operation. The simulation results are highlighting the flow fields at the collision region bounded between the wing and the ground. Sample of the simulation results is shown in Fig. 9.

The increment in lift is mainly resulted from the increased static pressure which creates an air cushion when the height decreases. This is leading to a ramming effect whereby the static pressure on the bottom surface of the wing is increased, leading to higher lift.

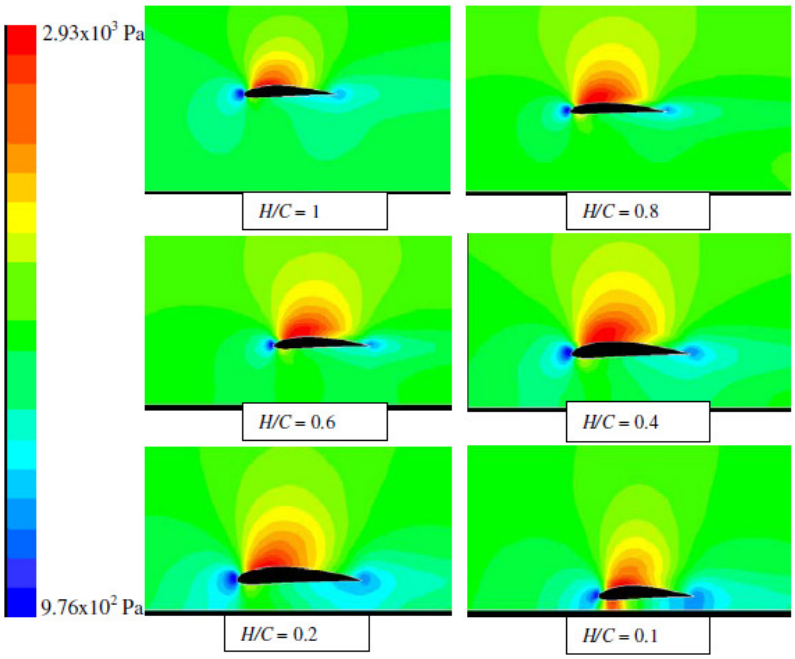

Fig. 9. Contours of the Dynamic Pressure around the Airfoil at Different *H/C* and at AOA = 0°.

6. Conclusions

The collision phenomena and its influence on the aerodynamic characteristics of wing operation near the ground were investigated experimentally and numerically. On the experimental part, a 2-D wing model having NACA4412 airfoil cross section was designed and fabricated using CNC facilities. A traverse mechanism was designed and fabricated to provide wing operation at different heights from the ground and different angles of attack. The experimental results were obtained by measurements in low speed wind tunnel. On the numerical part, the conservations of mass and momentum equations were solved by CFD using finite volume technique. To close the domain, the turbulence part of the flow was approximated by using RNG k-ε model. GAMBIT 2-4.6 software was used for modelling and FLUENT 6-3.26 software was used for the simulation. The aerodynamic parameters, lift, drag and pitching moment coefficients were measured experimentally and predicted numerically at various wing height from the ground.

The results were compared with previous works and good agreements were achieved. At a certain Reynolds number and AOA, it was found that the $C_{l.\ max}$ increases considerably as the wing approaches the ground. At Reynolds number of 4×10^5, the $C_{l.\ max}$ was increased by 8% when the height ratio, *H/C* reduced from 1 to 0.1. The increase in the inertia forces compared to the viscous forces, showed that the lift coefficient near the ground was affected considerably, compared to the change far away from the ground. At AOA = 4 and *H/C* = 0.1, the increase of the Re value from 10^5 to 4×10^5 causes the lift coefficient to increase by about 25%, while the drag was increased by about 80%. This gives indication that the take off and landing speeds are main contributor in the influence of the aerodynamic characteristics in the wing-ground collision phenomena.

Acknowledgment

The authors acknowledge Universiti Teknologi PETRONAS for granting the work under the Final Year Project funding scheme, and sponsoring the presentation of the paper in WEC2010. Special thanks are due to the Mechanical Engineering technicians, for their assistance during the use of the CNC facilities to produce the wing model, and the low speed wind tunnel to conduct the experimental measurements.

References

1. www.aerospaceweb.org (accessed 2009).
2. www.aerospaceweb.org/wingtip (accessed 2009).
3. Hsiun, C.; and Chen, C.K. (1996). Aerodynamic characteristics of a two-dimensional airfoil with ground effect. *Journal of Aircraft*, 33(2), 386-392.
4. Zerihan, J.; and Zhang, X. (2000). Aerodynamics of a single element wing in ground effect. *Journal of Aircraft*, 37(6), 1058-1064.
5. Zhang, X.; and Zerihan, J. (2003). Off-surface aerodynamic measurements of a wing in ground effect. *Journal of Aircraft*, 40(4), 716-725.
6. Firooz, A.; and Gadami, M. (2006). Turbulence flow for NACA 4412 in unbounded flow and ground effect with different turbulence models and two ground conditions. *International Conference on Boundary and Interior Layers*, University of Gottingen.
7. Ahmed, M.R.; Takasaki, T.; and Kohama, Y. (2007). Aerodynamics of a NACA4412 airfoil in ground effect. *AIAA Journal*, 45(1), 37-47.
8. Ahmed, M.R.; and Sharma, S.D. (2005). An investigation on the aerodynamics of a symmetrical airfoil in ground effect. *Experimental thermal and fluid science*, 29(2), 633-647.
9. Ahmed, M.R. (2005). Aerodynamic of cambered airfoil in ground effect. *International Journal of Fluid Mechanics Research*, 32(2), 157-183.
10. Molina, J.; and Zhang, X. (2010). Aerodynamics of an oscillating wing in ground effect. *Proceedings of the 48th AIAA Aerospace meeting including the new horizons Forum and aerospace Exposition, Orlando*, FL. 4-7 Jan (ISBN: 978-160086739-2); code 82585. Article no. 2010-0318.

11. Al-Kayiem, H.H.; and Aziat, M.N. (2008). Fabrication of NACA4412 airfoil model for wind tunnel tests by CAE. *Proceedings of 2nd Engineering Conference on Sustainable Engineering Infrastructures Development & Management*, Kuching, Sarawak, Malaysia.
12. Versteeg, H.K.; and Malaasekera, W. (2007). *An Introduction to computational fluid dynamics - The finite volume method*. (2nd Ed.), Pearson Education Limited, UK.
13. Fluent Incorporation, 2003, chapter10: Turbulence Modelling.